Vessel-platform automation: Integrating self assembly with configuration dependent control strategies

Bart Boogmans, Vittorio Garofano, Yusong Pang, Rudy Negenborn

November 2, 2021

Abstract

Modular waterborn stuctures, built from a set of smaller connected units, have shown recent developments to automate assembly and collaborative motion control. Future automated fleet control systems are envisioned to show formation of combined structures together with collaborative motion control approaches within a single framework to minimize human interaction over both operations.

A literature survey explored the state of the art on automated formation and control of modular waterborn structures, where the design spectrum has been broadened by characterizing approaches for more general 'reconfigurable' and 'collaborative' robotic systems. From this, a proof of concept has been developed of a modular fleet system performing automated assembly and collaborative motion control of an arbitrary configured structure, taking into account changing dynamics and network topology.

The developed framework proved able to assemble a set of single operating modules into a 3x1 lattice platform structure, with motion control in single vessel and assembled state adapting to the configuration at the time.

An approach on combining two systems (automated assembly & collaborative control) is presented throughout this paper supplemented with various insightsto aid further developments

Index Terms– Automation, Modular Vessel-Platform, Collaboration, Coordination, Motion-Control, Reconfiguration

1 Introduction

Advancing vehicle automation technologies allow, new or improved logistical applications in the maritime sector. Modular vessel systems, consisting of assembled waterborn units can compete to perform a niche of tasks where variable shape, rapid deployment and versitality are key. Structures assembled on water surface into platforms have seen explorative studies towards automation to reduce reliance on operators and potentially outperform them in some aspects. Automation of modular vessel-platforms could aid formation and motion of structures to, for instance carry arbitrary shaped objects or form ad-hoc infrastructure such as temporary bridges. Using the strength of modular, reusable components combined with low reliance on operators due to automation can form competitive solutions operating effectively with low resource consumption to a niche of logistical challenges.

O'hara et al. [8] and Paulos et al. [10] show development of an automated fleet of modules performing individual module motion and platform reconfiguration. The fleet is homogeneous where modules are identical and shaped rectangular at model scale with dimentions in the ratio of standard shipping containers. Modules connect via mechanical hook and rope actuators into a repeating lattice architecture [15]. O'hara et al. [8] approaches reconfiguration deterministically by distincting (1) generation of desired configuration, (2) selecting reconfiguration sequence, (3) positioning a module and (4) perform docking sequence.

Wang et al. [13] present a line of modular fleet systems named Roboat, where Amsterdam institute for Advanced Metropolitan Solutions (AMS) and Massachusetts Institute of Technology (MIT) are major contributors. The module design is based to form a framework upon which further tests can be performed for transportation and self-assembly to floating infrastructures, where model scale experiments pave the road towards full sized implementation [14]. Roboat vessels are used as a use-case by works that focus on various facets of modular vessel platform automation.

Park et al. [9] utilize a platform-centralized approach to control motion ofan arbitrary sized vessel-platform of Roboat modules. Control effort is generated by a PI controller running on one vessel that is elected as coordinator, which subsequently allocates effort between actuators on the modules. This centralized platform control system can be classified in terms of Guidance, Navigation and Control (GNC) [1], where the platform motion-controller is fed reference pose (position and orientation) as input from a planning (guidance) layer and performs a state estimation (navigation). An approximate platform model is estimated based on the number of connected modules to adapt the control-effort generation subsystem to arbitrary configura-

tions.

Mateos et al. [7] shows development of a latching system consisting of male/female ball/cone components for assembling Roboat vessels, discusing latching hardware and experimental results. Gheneti et al. [3] and Kelly [5] present trajectory planning algorythms for reconfiguration of modular surface structure components. The proposed core logic of the shapeshifting algorythm is finding the largest overlap between current and desired configuration. Gheneti et al. [3] show approaches and experimental results of platform shapeshifting, distincting the whole reconfiguration problem into (1) task planning, (2) trajectory planning and (3) trajectory tracking.

Literature survey showed no information on a modular fleet system incorporating automated reconfiguration (Fig. 1) with collaborative configuration dependent control strategies (Fig. 2) in a single framework, thus consequences of integrating the two behaviors in a single system appear unmapped. It would be useful for developers to know what system requirements, characteristics and constraints emerge from such integration, as this information can be used to make well informed, effective, scalable, interoperable and long term beneficial design choices. Gathering and documenting approaches and experiences on integration can pave the road towards effective implementations to fully benefit from automated structure assembly while motion control of the combined platforms are enhanced by effective collaborative approaches.

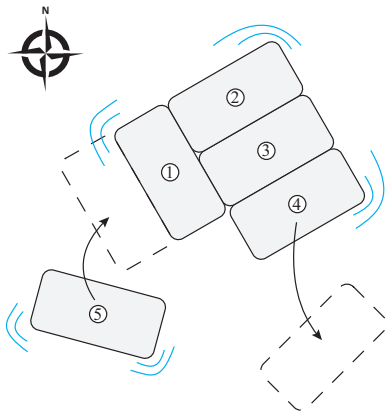

Figure 1: Automatic reconfiguration of a vessel platform. Module (1)-(4) are connected. (4) disassembles. (5) approaches for assembly.

A framework is proposed to control a multi-robot fleet simultaneously performing automated assembly into platforms and collaborative, coordinated motion control using Delfia-1* model scale vessels (Fig. 3). The framework should support arbitrary configurations, as this creates versatility to a wide set of tasks for modular vessel platforms

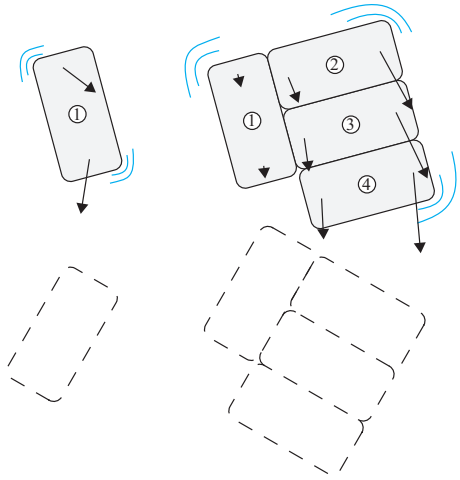

Figure 2: Multi-robot vessel platform motion control collaboration and coordination shown on two configurations. Arrows illustrate forces generated by thrusters.

as a key element supporting commercial competitivity. Solutions are designed to be modular, such that subsystems are conveniently swapped out others (perhaps improved and better performing), stimulating further improvements and reusability of work. The goal of this design is not to optimize an existing system, but to explore a novel combination of behavioral concepts that is expected to be of interest in the near future.

Guidance (including reconfiguration planning), navigation and motion control tasks are distributed to components of a multi-agent network. Motion control structure is centralized per platform, where network-topology varies throughout operation as configurations change. Control effort generation and allocation are distinct subsystems, where the former uses a proportional, integral and differential (PID) control approach adapting to predicted platform dynamics. Platform-models are estimated by combining models of individual modules while taking into account relative placement and orientation. This approach aims to provide a framework for predicting with reasonable accuracy over arbitrary shapes as a quick, cheap and scalable solution with respect to parameter estimation experiments on all configurations.

Design, implementation and evaluation of the developed system is discussed throughout this paper, where section 2 explains control structure, subsystem division and variable network-topology with high level perspective. Section 3 zooms down to discuss design and implementation of each subsystem. Performance of the overall system is evaluated in section 4, after which section 5 concludes.

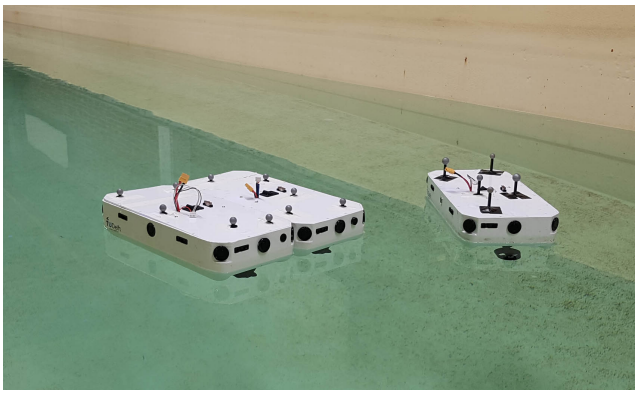

Figure 3: Three Delfia-1* modules from Researchlab Autonomous Shipping (RAS) Delft in the towing tank of TUDelft department of Maritime and Transport Technology (MTT)

2 Multi-Vessel Control Structure

Goal of the developed system is showing simple automation of both reconfiguration and collaborative platform motion control. Distinction of functions according to GNC scheme logic is used to categorize subfunctions. The extra function of assembly planning is integrated withing the guidance layer.

2.1 Network Topology

The control structure operates in three layers, depicted in figure 4. The concept of a 'platform' and a corresponding centralized platform-controller are key to the functioning of this system.

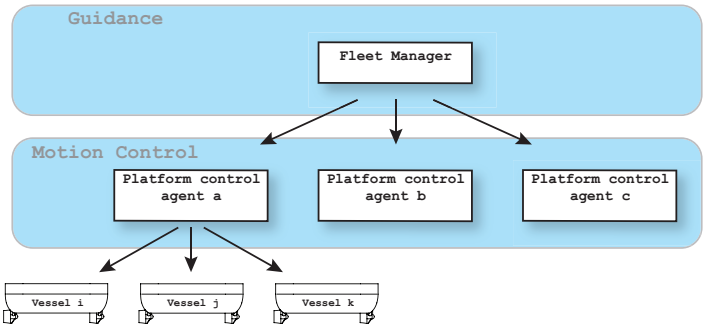

Figure 4: Hierarchical network topology, where platform control agents each manage a unique set of modules.

A guidance layer coordinates motion planning and the assembly processes, which is implemented as a single fleet-manager entity operating as a rather simplistic state machine cycling trough phases due to system triggers or operator input. Other setups for guidance layer funcionality (such as proposed by [8] [10] [3] [5]) could be applied to the approach of integrating collaborative motion control with self-assembly as presented in this paper.

Tasks generated by the fleet manager are passed to Platform-controllers, each managing motion control of a set of connected modules in a centralized fashion. This platform controller uses a reference state and a platform-state estimation to generate actuator responses for all modules which are sent to the corresponding modules. The platform controlling agent can be embodied by a computer anywhere on the network (on a module, on shore or distributed) with sufficient computational power and the network reliability.

The amount of modules that an platform-control-agent manages varies over time as vessels attach or disconnect. Thus all functions of the platform controller need to be able to handle a variable amount of modules and configurations. Changes in configuration affect control structure topology, as module ownership is transferred between platform controlling agents during reconfiguration (for example, the network topology shown in Fig 4 would have ownership of disassembling vessel k move from platform controller a to b).

Communication between agents is facilitated through WiFi and the Robotic Operating System (ROS) as middleware in an interoperable and modular way thanks to its publisher-subscriber protocols, which allows a variable amount of agents to listen (subscribe) and send (publish) to various organised datastreams (topics).

2.2 Multi-agent Control approach

State of vessels are described in line with conventions of SNAME [12] as shown in table 1, and illustrated in figure 5.

DOF	Positions, Orientations	Velocities	Forces, Moments
Surge	x	u	X
Sway	y	v	Y
Heave	z	w	Z
Roll	ϕ	p	K
Pitch	θ	q	M
Yaw	ψ	r	N

Table 1: SNAME vessel state notation

Vessel motion in simplified to three degrees of freedom on the surface plane (x,y and yaw), in which a platform coordinate system $\{p\}$ is defined that has constant placement relative to connected modules (Fig. 6).

Control objective is generated by a guidance system as time varying position with preprogrammed protocols to provide platform motion control layer with a reference state. Platform reference state is noted as

$$x_{ref} = \eta_{p,ref} = \begin{bmatrix} \mathbf{p}_p^n \\ \Theta_{np} \end{bmatrix} = \begin{bmatrix} x_p^n \\ y_p^n \\ \Psi_p^n \end{bmatrix} \quad (1)$$

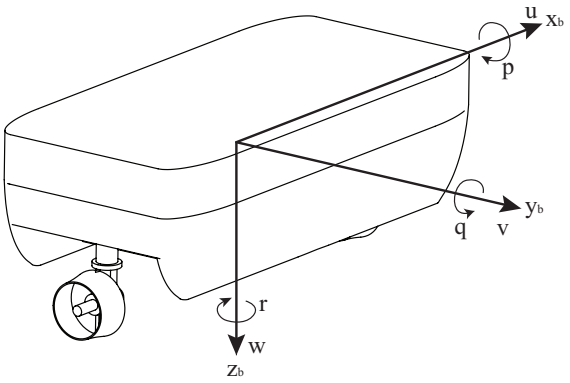

Figure 5: Six degrees of motion of a Delfia vessel expressed with respect to the body-fixed coordinate system $\{b\}$

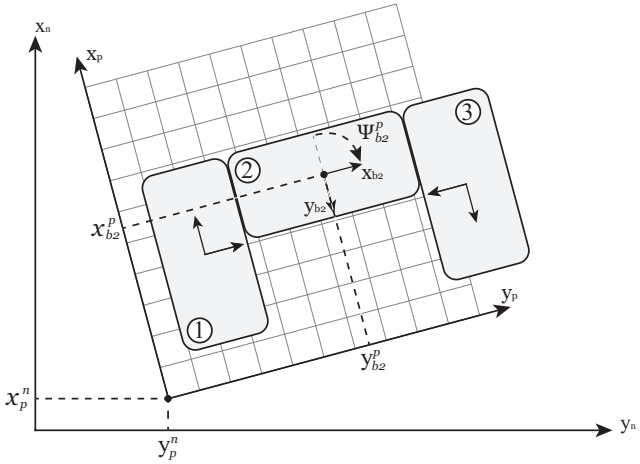

Figure 6: An assembly of three connected vessels, illustrating interpretation of global ($\{n\}$), platform ($\{p\}$) and module ($\{b\}$) coordinate systems.

where η_p, ref is a vector describing vessel pose, including positions in vector $\mathbf{p}_p^n$ and angles in vector Θ_{np} of which elements are shown for three DOF surface motion. Platform motion control is based on state feedback, with the control loop illustrated in Fig. 7. Platform state is estimated by trasposing measured position of modules according to module placement within the platform coordinate system. Control effort generation and allocation are distinct where the former uses an estimated model to adapt actuator behavior to maintain performance while the system dynamics change.

Used modules are rectangular Delfia-1* vessels, equipped with two rotating azimuth thrusters, forming a homogeneous fleet. Delfia-1* modules have two axes of symmetry in hull shape, weight distribution and thruster placement. The vessel's body fixed coordinate system origin is defined in the middle, where planes of symmetry coincide.

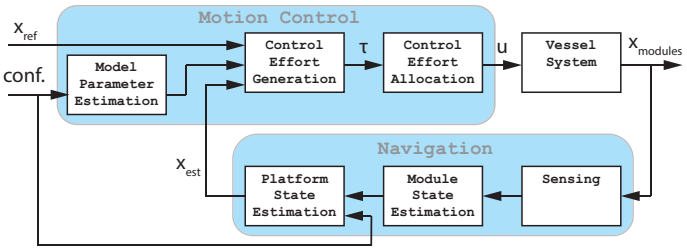

Figure 7: A schematic showing the platform motion control feedback loop.

3 Subsystems

System components as described in Sec. 2 and illustrated in Fig 4 and 7 each had a solution picked as explained here.

3.1 Guidance & Navigation

Modules assemble in lattice formation, using active magnets to remain configured. Task execution, including motion guidance and assembly operates in a static preprogrammed phasewise fashion. Automated configuration of a 3x1 configured platform is illustrated in Fig. 8, where connection phases consist of (1) initial line-up, (2) movement to connection site, (3) evaluation of succesful assembly by operator, (4) change of control topology to match new configuration and (5) adjust platform control behavior to new configuration.

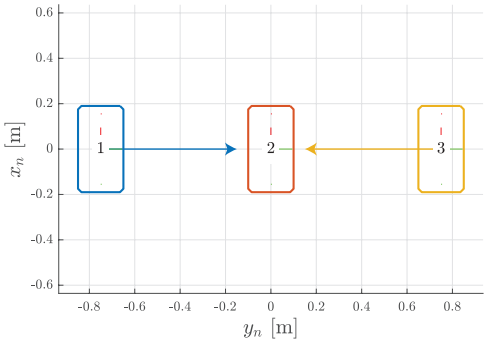

Figure 8: Simple platform assembly protocol from top vieuw. Vessel 1 and 3 are lined up to approach connecting to vessel 2 on either side. Once connectors are within range, the magnets snap into place, fixing relative motion.

Early test yielded modules floating around the connection site unconstrained in three degrees of motion, resulting in unpractically long connection times. This was solved by using normal forces on the modules' hulls to align surfaces, being a common trick used by human controlled ships (such as docking ferries). Fig. 9 shows how references of approaching modules overlapping with docking station (in this case another module) yield a small normal force be-

tween vessels, ensuring that they keep making contact, and avoid rotation. Reconfigured platforms are controlled by a

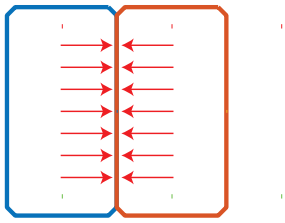

Figure 9: Normal forces that result from overlapping references during assembly.

single platform-controller with new configuration, network topology and control approach to reach motion-control objectives of logistical tasks as given by the guidance layer.

The navigation system aims to estimate the platform state, which is actually but a concept to represent a collection of modules and is not directly measurable. It is however estimated by using a feedback signal of module positions aquired over through an on-shore optical tracking system, and module's known, constant placement within the body. An OptiTrack^{TM} optical motion tracking system uses ceiling mounted cameras and infra red reflectors (grey balls visible on top of Delfias in Fig. 3), to localize modules. Consider an update of the position and orientation of a module as

$$\eta^n_{b/n} = \begin{bmatrix} \mathbf{p}^n_{b/n} \\ \Psi_{b/n} \end{bmatrix} = \begin{bmatrix} \mathbf{x}^n_{b/n} \\ \mathbf{y}^n_{b/n} \\ \Psi_{b/n} \end{bmatrix} \tag{2}$$

where $\eta^n_{b/n}$ is the pose of body (module) b with respect to the origin of inertial frame $\{n\}$, expressed in $\{n\}$. The placement of all modules (defined by the position and orientation of module's body fixed coordinate system $\{b\}$) within the assembly is known and can be described with respect to $\{p\}$ expressed in $\{p\}$ as

$$\eta^p_{b/p} = \begin{bmatrix} \mathbf{p}^p_b \\ \Theta_{pb} \end{bmatrix} \tag{3}$$

altough, instead of euler angles Θ_{pb}, the rotation matrix $\mathbf{R}^p_b$ from coordinate system $\{b\}$ to $\{p\}$ can also be used to express relative orientation. Interpretation of pose expressed in platform frame is illustrated in Fig. 6. Measured module pose is transformed to platform pose by subsequent rotation and translation. For the three considered degrees of surface plane motion the platform state becomes

$$\eta^n_{p/n} = \begin{bmatrix} \mathbf{p}^n_{p/n} \\ \Psi_{p/n} \end{bmatrix} \tag{4}$$

where

$$\Psi_{p/n} = \Psi_{b/n} - \Psi_{b/p} \tag{5}$$

and

$$\mathbf{p}^n_{p/n} = \mathbf{p}^n_{b/n} - \mathbf{p}^n_{b/p} = \mathbf{p}^n_{b/n} - \mathbf{R}(\Psi_{p/n})\mathbf{p}^p_{b/p} \tag{6}$$

3.2 Model parameter estimation

The control approach uses the concept of an approximate platform-model to then influence motion control behavior similar to Park et al. [9], yet also taking into account platform shape besides number of connected modules. Module-connectivity and dynamical models of individual modules are known, and are used to form a single platform model assuming rigid connections. Use-cases where vessel assemblies are formed in many varying configurations can make experimental model parameterization infeasible for all reasonably forseeable configurations, where prediciont of a dynamical model by combining models of modules can provide a quick, cheap and scalable solution.

A dynamic model of the platform is formed by expressing all models of the modules in identical generalized coordinates that describe platform state. By describing module motion and forces in coordinate system and origin of $\{p\}$, resultants can be summed. It is shown how terms from multiple module models can be grouped for convenient expression, and how subsequently the combined structure's centre of mass can be found.

Models of modules are expressed in platform frame origin by (1) translating the expressions to o_p as a reference point and (2) rotating the expressions to match coordinate system $\{p\}$. This approach works also for models of which the origonal inertial matrix is not defined in the CG, and/or for models that have directional dependent mass (e.g., hydrodynamic added mass).

Generalized positions and velocities of the platform are described respectively as

$$\eta^n_{p/n} = \begin{bmatrix} \mathbf{p}^n_p \\ \Theta_{np} \end{bmatrix} \tag{7}$$

$$\nu^p_{p/n} = \begin{bmatrix} \mathbf{v}^p_{p/n} \\ \omega^p_{p/n} \end{bmatrix} \tag{8}$$

The assembly is considered rigid, thus there is no motion between modules, making relative velocity of a module expressed in rotating frame $\{p\}$ zero (if derivative is taken in rotating, non-inertial frame$\{b\}$ or $\{p\}$)

$$\nu^p_{bi/p} = \nu^p_{bi/bj} = \begin{bmatrix} \mathbf{v}^p_{bi/p} \\ \omega^p_{bi/p} \end{bmatrix} = 0 \tag{9}$$

and

$$\frac{d}{dt}\mathbf{R}^p_b = 0 \tag{10}$$

Velocities and generalized forces can be converted to vector notation as

$$\nu^b_{b/n} = \begin{bmatrix} \mathbf{v}^b_{b/n} \\ \omega^b_{b/n} \end{bmatrix} = \mathbf{J}^b_p \mathbf{H}(\mathbf{p}^p_{b/p}) \nu^p_{p/n} \tag{11}$$

$$\begin{aligned} \tau^p_p = \begin{bmatrix} \mathbf{f}^p_p \\ \mathbf{m}^p_p \end{bmatrix} &= \begin{bmatrix} \mathbf{R}^p_b \mathbf{f}^b_b \\ \mathbf{R}^p_b (\mathbf{m}^b_b + \mathbf{p}^b_{p/b} \times \mathbf{f}^b_b) \end{bmatrix} \\ &= \begin{bmatrix} \mathbf{R}^p_b & 0 \\ 0 & \mathbf{R}^p_b \end{bmatrix} \begin{bmatrix} \mathbf{I} & 0 \\ \mathbf{S}(\mathbf{p}^b_{p/b}) & \mathbf{I} \end{bmatrix} \begin{bmatrix} \mathbf{f}^b_b \\ \mathbf{m}^b_b \end{bmatrix} \\ &= \mathbf{J}^p_b \mathbf{H}^\top(\mathbf{p}^b_{p/b}) \tau^b_b \end{aligned} \tag{12}$$

where coordinate system transformation between rotated frames $\{p\}$ and $\{b\}$ is done by operator

$$\mathbf{J}^p_b = \begin{bmatrix} \mathbf{R}^p_b & 0 \\ 0 & \mathbf{R}^p_b \end{bmatrix}, \quad \mathbf{J}^{p\top}_b = \begin{bmatrix} \mathbf{R}^p_b & 0 \\ 0 & \mathbf{R}^p_b \end{bmatrix} \tag{13}$$

and translation of forces is represented by operator [1]

$$\begin{aligned} \mathbf{H}^\top(\mathbf{p}^b_{p/b}) &= \begin{bmatrix} \mathbf{I} & 0 \\ \mathbf{S}(\mathbf{p}^b_{p/b}) & \mathbf{I} \end{bmatrix} \\ \mathbf{H}(\mathbf{p}^b_{p/b}) &= \begin{bmatrix} \mathbf{I} & -\mathbf{S}(\mathbf{p}^b_{p/b}) \\ 0 & \mathbf{I} \end{bmatrix} \end{aligned} \tag{14}$$

and $\mathbf{S}(\mathbf{x})$ is the 3x3 cross product matrix operator. Motion of an individual rigid body can be described in $\{b\}$ as [1]

$$\mathbf{M}\dot{\nu}^b_{b/n} + \mathbf{C}(\nu^b_{b/n})\nu^b_{b/n} = \tau_{res} \tag{15}$$

where $\mathbf{M}$ represent inertia of the rigid body and constant hydrodynamic added mass, $\mathbf{C}(\nu^b_{b/n})\nu^b_{b/n}$ represent coriolis and centripetal forces and τ_{res} are the resultant forces on the body.

Coriolis and centripetal forces arise due to the rotation of $\{b\}$ with respect to the inertial frame, and are fully determined by the inertial matrix. Fossen [1] shows how an energy approach, using Kirchhoff's equations is a convenient way to find the coriolis and centripetal matrix. If kinetic energy of vessel and added mass is written in quadratic form Kirchhoff [6]

$$\mathbf{T} = \frac{1}{2} {\nu^b_{b/n}}^\top \mathbf{M}^b \nu^b_{b/n} \tag{16}$$

where inertial matrix and velocities are described in $\{b\}$, and inertial matrix $\mathbf{M}^b$ represent rigid body inertia and hydrodinamic added mass. Substituting Eq. 11 gives

$$\mathbf{T} = \frac{1}{2} {\nu^p_{p/n}}^\top \mathbf{H}^\top(\mathbf{p}^p_{b/p}) {\mathbf{J}^b_p}^\top \mathbf{M}^b \mathbf{J}^b_p \mathbf{H}(\mathbf{p}^p_{b/p}) \nu^p_{p/n} \tag{17}$$

Which can be rewritten as

$$\mathbf{T} = \frac{1}{2} {\nu^p_{p/n}}^\top \mathbf{M}^p \nu^p_{p/n} \tag{18}$$

where the inertial matrix of a module is expressed in platform coordinates as

$$\mathbf{M}^p = \mathbf{H}^\top(\mathbf{p}^p_{b/p}) {\mathbf{J}^b_p}^\top \mathbf{M}^b \mathbf{J}^b_p \mathbf{H}(\mathbf{p}^p_{b/p}) \tag{19}$$

Equation 18 can be substituted in Kirchhoff's vector equations [6]

$$\frac{d}{dt}\left[\frac{\partial \mathbf{T}}{\partial \nu_1}\right] + \mathbf{S}(\nu_2)\frac{\partial \mathbf{T}}{\partial \nu_1} = \tau_1 \tag{20}$$

$$\frac{d}{dt}\left[\frac{\partial \mathbf{T}}{\partial \nu_2}\right] + \mathbf{S}(\nu_2)\frac{\partial \mathbf{T}}{\partial \nu_2} + \mathbf{S}(\nu_1)\frac{\partial \mathbf{T}}{\partial \nu_1} = \tau_2 \tag{21}$$

where $\nu_1 = \mathbf{v}^p_{p/n}$, $\nu_2 = \omega^p_{p/n}$, $\tau_1 = \mathbf{f}^p_p$ and $\tau_2 = \mathbf{m}^p_p$ to obtain the equations of motion of a module expressed in platform coordinates. Notice that the expression of inertial matrix in Eq. 19 is constant, due to rigid body assumptions. This allows formation of the (tranlated and rotated) dynamical model in a 'normal' fashion, such as shown in Fossen [1], where terms that are not dependent on accelleration, but on velocity are grouped to form the coriolis-centripetal matrix, which can be represented in many forms. Various works describe options parameterizations such as skew-symmetric Sagatun and Fossen [11] or velocity independent Fossen and Fjellstad [2], which can be chosen to best suit a project.

Forces on modules can be summed to find resultant force on the complete platform, given that they are expressed in the same point and coordinate system. If n connected modules generate a generalized force τ_{bi} expressed in the same point and coordinate system, the forces can be added to find the total force for the entire platform as

$$\tau^p_p = \sum_{i=1}^{n} \tau^p_{bi} \tag{22}$$

Which can allow convenient reformulation of a total model. Grouping of terms allows expression of 'platform inertia', 'total dampening' or 'total control-effort', to name only some. For instance, expressing inertia of various modules in a the same platform coordinates allows us to express total platform-inertia

$$\begin{aligned} \mathbf{M}^p_p &= \sum_{i=1}^{n} \mathbf{M}^p_{bi} \\ &= \sum_{i=1}^{n} \mathbf{H}^\top(\mathbf{p}^p_{bi/p}) {\mathbf{J}^{bi}_p}^\top \mathbf{M}^{bi}_{bi} \mathbf{J}^{bi}_p \mathbf{H}(\mathbf{p}^p_{bi/p}) \end{aligned} \tag{23}$$

where $\mathbf{M}^p_p$ is the platform inertial matrix, $\mathbf{M}^p_{bi}$ is the inertial matrix of module i expressed in $\{p\}$. This expression can conveniently be used to compute terms regarding coriolis and centripetal forces for the complete platform in one go as one would do with a single vessel, instead of obtaining it by summating the coriolis and centripetal components of all modules.

Other forces from individual modules, such as to dampening, can be integrated to a platform model similar to accelleration dependent coefficients as shown, by expressing in the same point and coordinate system.

From the expression of total platform inertial tensor as Eq. 23 we can find the centre of gravity of the platform. Recall that the centre of gravity is the point of a rigid object, if a (gravitational) force is applied, this force creates no resultant torque, and thus no angular accelleration. This effectively means that if we find the position of platform centre of gravity $\mathbf{p}_g$, and express our platform model in that point (similar as in Eq. 19), no coupling between rotation and translation should exist in the inertial matrix. Expressing the inertial matrix in CG_p can be done by:

$$\mathbf{M}_p^{CG} = \mathbf{H}^\top(\mathbf{p}_{g/p}^p)\mathbf{M}_p^p\mathbf{H}(\mathbf{p}_{g/p}^p) \tag{24}$$

No coupling in $\mathbf{M}_p^p$ between rotation and translation means that the off-diagonal quadrants are zero, thus if

$$\mathbf{M} = \begin{bmatrix} \mathbf{M}_{11} & \mathbf{M}_{12} \\ \mathbf{M}_{21} & \mathbf{M}_{22} \end{bmatrix} \tag{25}$$

then

$$\mathbf{M}_{12}^{CG} = \mathbf{M}_{21}^{CG} = 0_{3x3} \tag{26}$$

evaluating the resulting upper right quadrant of Eq. 24 and 26 gives

$$\mathbf{M}_{CG,12} = \mathbf{M}_{p,12} - \mathbf{M}_{p,11}\mathbf{S}(\mathbf{p}_g^p) = 0_{3x3} \tag{27}$$

$$\mathbf{S}(\mathbf{p}_g^p) = {\mathbf{M}_{p,11}}^{-1}\mathbf{M}_{p,12} \tag{28}$$

which allows us to easily extract the center of mass for the combined structure by substituting known inertial parameters and solving for $\mathbf{p}_g^p$.

It can be debated whether the summation of individual ship dynamic models sufficiently represents overall stucture dynamics. Humphreys and Watkinson [4] stated (about individually operating vessels) that forces and moments represented by acceleration hydrodynamic coefficients can, to a very great extent, be modeled as potential flow phenomena. Yet platforms have vessels operating in very close proximity, which might significantly affect the boundary layer size and shapes. This can affect terms representing added mass and dampening both positively and negatively.

3.3 Control effort generation

The control block is based on a Proportional-Integrator-Differential (PID) controller, designed to scale to estimated model parameters. Three parralel controllers are used to control each individual degree of freedom, as illustrated in 10

Control gains of the control-effort-generation block are designed to scale such that, once tuned for a single configuration, show similar behavior for any other configuration or platform size. For this, the following configuration dependent parameters are used.

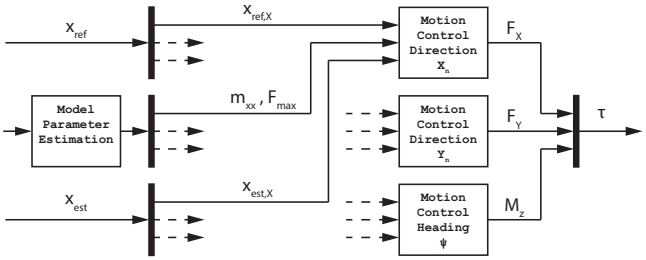

Figure 10: Parralel platform motion controller setup showing signal flow to motion control block for x_n direction, parsing reference (X_{ref}), model parameters and state (X_{est}) to generate desired control effort (τ)

The centre of mass of the platform is found using Eq. 28. It can then be substituted in Eq. 24 to express the equations of motion in that particular point. For three degrees of freedom in the surface plane this becomes shaped as

$$\mathbf{M}_p^{CG} = \begin{bmatrix} m_{xx} & m_{xy} & 0 \\ m_{yx} & m_{yy} & 0 \\ 0 & 0 & I_{zz} \end{bmatrix} \tag{29}$$

where

$$\mathbf{M}_{11} = \begin{bmatrix} m_{xx} & m_{xy} \\ m_{yx} & m_{yy} \end{bmatrix} \quad \mathbf{M}_{12} = \begin{bmatrix} 0 \\ 0 \end{bmatrix}$$

$$\mathbf{M}_{12} = \begin{bmatrix} 0 & 0 \end{bmatrix} \qquad \mathbf{M}_{22} = I_{zz}$$

Which shows the estimated moment of inertia I_{zz} in the bottomright corner. If modules have hydrodynamic added mass being modelled as a constant, direction-dependent constant, the off-diagonal elements m_{xy} and m_{yx} may be nonzero. This can also result that masses in xx and yy direction may be unequal, which can feel rather counter intuitive, as this is never the case with normal rigid body motion. The cause of this still originates from the origonal form of module inertia matrix, as this inherited by using such models.

The controllers responsible for linear motion will use an estimation of the mass of the platform. Rotating the inertial matrix can be done such that the off diagonal elements m_{xy} and m_{yx} become zero. The magnitude of the diagonal elements can be easily found, as they are the eigenvalues of M_{11}. The average of the eigenvalues is used as the estimated omni-directional mass for adapting controller behavior. For

linear motion in 2 degrees of freedom (x and y) this becomes

$$m_p \approx \frac{1}{2} \sum Eig(\mathbf{M}_{11}) \tag{30}$$

As the fleet utilizes rotatable azimuth thrusters, the maximum force is generated by the propellers on full power in a single direction. The maximum force that the platform can generate can be found by summation of maximum thruster force of all thrusters

$$\mathbf{f}_{p,max} = \sum_{i=1}^{n_{thr}} f_{i,max} \tag{31}$$

where n_{thr} refers to the total amount of thrusters, and $f_{i,max}$ is the maximum force that the ith propeller can supply. The homogeneous fleet has two identical propellers per module, such that.

$$\mathbf{f}_{p,max} = 2 * n * f_{prop,max} \tag{32}$$

Maximum torque is generated when all thrusters supply maximum force in the direction perpendicular to a vector between CG and the thruster. For a single vessel, this becomes

$$\mathbf{m}_{i,max} = |\mathbf{r}| f_{i,max} = |\mathbf{p}^p_{CG/p} - \mathbf{p}^p_{thr,i/p}| f_{i,max} \tag{33}$$

where $\mathbf{p}^p_{CG/p}$ is the position vector of the platform CG and $\mathbf{p}^p_{thr,i/p}$ is the position of the ith thruster. The latter is usually given in local frame of a module, but can be converted to platform coordinates by matrix rotation and a translation as:

$$\mathbf{p}^p_{thr,i/p} = \mathbf{R}^p_{bj} \mathbf{p}^{bj}_{thr,i/bj} + \mathbf{p}^p_{bj/p} \tag{34}$$

where $\mathbf{p}^{bj}_{thr,i/bj}$ is the position of thruster i, mounted on module j, expressed in the body fixed coordinate system of module j. $\mathbf{p}^p_{bj/p}$ is the position of module j expressed in platform coordinate system. Summation of Eq. 33 over all modules yields total maximum torque generated by actuators for a given configuration as

$$\mathbf{m}_{p,max} = \sum_{i=1}^{2n} \mathbf{m}_{i,max} \tag{35}$$

It should be noted that the Eq. 32 and 35 show absolute maxima, which need full participation of all actuators to be reached. These maxima can not be obtained in different degrees of motion simultaneously, as outputs will be saturated. To avoid unpredictable control effort generation, actuator operation near output saturation is avoided during implementation.

The control gains of the three parralel PID controllers are tuned to a single reference configuration. As the configuration changes the control gains will adapt to the newly estimated dynamics. The control gain scaling is based on the assumption that a configuration will have a response comparable to the reference, but in a different time scale. Typical errors that are fed into PID gains will thus be of comparable magnitude. System responses of current and reference configurations are thus aimed to be approximately comparable such that

$$\eta_c(t) \approx \eta_{ref}(C * t) \tag{36}$$

If control forces are a dominant factor to the response time of a step input on the system, a characteristic accelleration of a configuration can be defined as

$$a = \frac{Force}{Inertia} \tag{37}$$

This is used to estimate the time scaling factor is estimated as the ratio of maximum accelleration of a configuration with respect to the reference configuration.

$$C_c = \frac{a_c}{a_{ref}} = \frac{F_c \; I_{ref}}{F_{ref} \; I_c} \tag{38}$$

where a_c and a_{ref} are the characteristic accellerations of the current and reference configuration respectively.

All gains is designed to scale to the maximum obtainable control effort. The base value of contribution is determined in the gain tuning process of the reference configuration. The eventual output of any proportional integral and derivative gains is multiplied by the maximum control effort in that dimention.

Output of the control effort from proportional gain scales to the magnitude of the error, which assumed comparable in all configurations. This could result in, for example, a proportional gain that is to contribute 60% of the maximum obtainable control effort at an error of $e = 1.0$. The gain would become

$$K_p = K_{p,base} * \tau_{max} = 0.6 * \tau_{max} \tag{39}$$

such that the control effort contributed by the proportional block becomes

$$\tau_{i,prop} = e * K_p = 0.6 * \tau_{max} \tag{40}$$

Integral control is however affected by the time in which the system responds. A system that responds slower ($C_c < 1$) than the reference configuration will encounter additional integrator buildup. Time factor C_c compensates for change of integrator output due to response time by adjusting integral gain as

$$K_i = C_c \; K_{p,base} \; \tau_{max} \tag{41}$$

such that integral control output becomes

$$\tau_{i,int} = K_i \int_0^t e \; dt = C_c \; K_{p,base} \; \tau_{max} \int_0^t e dt \tag{42}$$

Derivative control output is also affected by time, but scales inversely to time factor C_c with respect to integral

control. Imagine, for example, a mass (*cough* *cough* vessel) that approaches the reference state, which would make the time derivative of the error negative. Derivative control would attempt to slow the mass down as it approaches it's desired state to avoid overshoot. An object, such as a container vessel, with low maximum control forces relative to the large mass would have to use take this speed more serious than highly manouverable vessels. Derivative adapts to a configuration as

$$K_i = \frac{K_{d,base}\ \tau_{max}}{C_c} \tag{43}$$

Base values of controller gains ($K_{p,base}$,$K_{i,base}$,$K_{b,base}$) will be set while revieuwing responses of the system in reference configuration. A PID controller can be manually tuned, or with the help of many tools such as automated PID tuning software. Linear motion in x and y direction will have identical control settings, as dependency on the orientation of reference frame $\{n\}$ is considered undesirable.

3.4 Control effort allocation

Control effort, as shown in the previous section, needs to be allocated onto the platform's actuators. The amount of thrusters available varies per configuration. Also placement and orientation of actuators can differ. A platform needs to be able to sufficiently control it's motion in all reasonably forseeable configurations. As the amount of different configurations is rather large, a general solution is used, that can solve the control effort allocation problem for all possible configurations. The designed control effort allocation protocol relies on the following main principle: "The contribution of an actuator to a desired resulting force or moment is proportional to its ability to contribute relative to that of the combined set of actuators."

This principle manifests particularly in rotational motion, as the ability of a thruster to generate torque relies on its placement with respect to the centre of gravity. Linear motion turns out not to exhibit such dependencies, as all thrusters are equal in strength, and possible orientation. To compute actuator commands that satisfy the desired control effort, it is allocated in each degree of freedom individually and finally combined.

Collaborative distribution of control effort was aimed to perform in a coordinated fashion. Fig.11 shows various independent and combined modes of motion in 3x1 assembled configuration, illustrating how the control allocation protocol assigns tasks to actuators using the described method.

4 Results

4.1 Assembly

Performance of reconfiguration will be quantified by evaluating the change in relative pose between neighbouring modules in all considered degrees of freedom. Pose of vessel j with respect to vessel i expressed in the body fixed coordinate system of vessel i is expressed as:

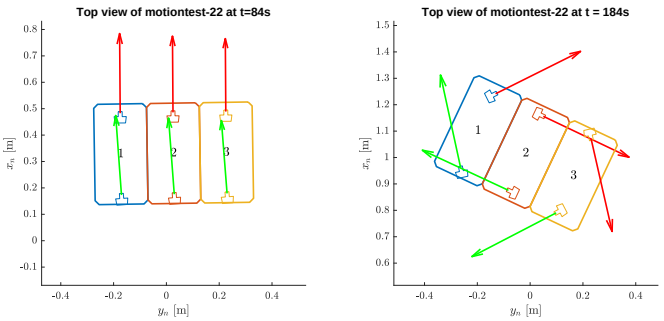

Figure 11: Control effort allocated to create (almost) pure force in x direction (left) and torque (right).

$$\eta_j^i = \begin{bmatrix} \mathbf{p}_j^i \\ \Theta_{ij} \end{bmatrix} = \begin{bmatrix} x_j^i \\ y_j^i \\ \Psi_j^i \end{bmatrix} \tag{44}$$

Assembly succes or failure was easily detectable by eye, but can be supported quantitatively by evaluating relative motion. The two modules attempted assembly simultaneously which is shown in Fig.12.

The signals showing relative positions in Fig.13 show forms of plateauing behavior, which is particularly interesting. The slope of these signals becoming a plateau means that relative speed has suddenly become near zero. This is considered to be due to physical contact between hulls. This can be a bump, soft contact, or a connector snapping two modules together. Relative pose of both connecting modules show some similarities. Pose in various DOFs show plateaus where the speed suddenly becomes near zero, which are most clear in y direction for both modules. Furhermore, a clear moment can be observed on which relative motion becomes near zero for not one, but all degrees of motion, indicating a succesful connection.

Figure 13 illustrate how the relative motion was interpreted for module 1 at two different timestamps. At $t = 308s$ rapid descelleration, is visible in y direction due to hull contact, while vessel 1 is still misaligned. Some motion and aligning occurs until relative motion suddenly halts, around $t = 364s$. This shows the connector performing to restrain relative motion in configured state, as all degrees of motion come to a halt instantaneous.

To further quantify the remaining perceived motion after assembly of module 1, the dataset is evaluated from the moment of connecting (approximately at $t = 364$) and 10 seconds thereafter.

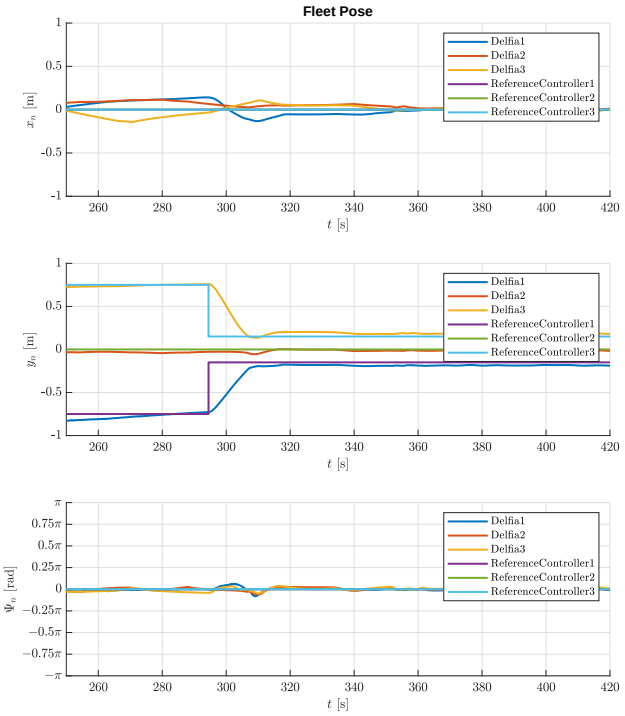

Figure 12: Module position plotted versus time, during the platform assembly stage. Vessels are initially lining up side-by-side, until they approach due to changin y reference values.

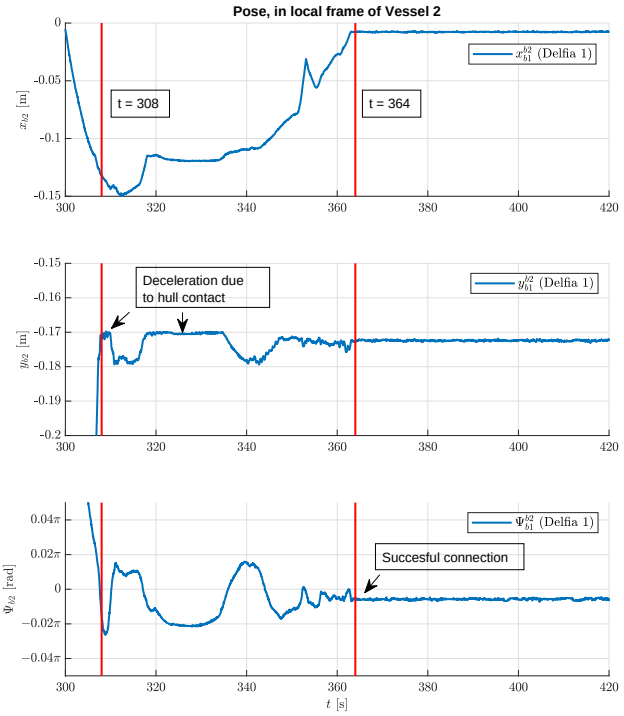

Figure 13: EvaluationConnectTwoInstancesAllDofs

		Average	Minimum	Maximum	maxAmpl	Variance
x	[m]	-0.0076628	-0.0082233	-0.0071825	0.0010408	4.3663e-08
y	[m]	-0.17236	-0.17288	-0.17198	0.00089951	2.6465e-08
Ψ	[rad]	-0.018446	-0.02136	-0.014622	0.006738	1.0167e-06

Table 2: Relative motion of module 1 with respect to body-fixed frame of module 2 for $364 < t < 374$.

4.2 Motion control

To evaluate the motion control performance of the developed framework, vessel system will be tasked to follow a time varying reference signal with step changes. Performance quantification is done by expressing rise-time and settling-time and overshoot of step responses to reference position of the platform in all considered degrees of freedom. Thoughout experiments steps in the platform's reference pose are given in one degree of freedom at a time.

Correctness of using the assumption of the used timescale can be evaluated by comparing response times of reference and assembled configuration. This will show to what extent the system maintains similar behavior over changing configurations, which will give indicators how it might behave for other configurations.

Firstly, the system is required to perform automated vessel platform reconfiguration. This criteria is reached as has been observed throughout operation (by seeing magnet connectors snap into place), yet this is quantitatively supported by expressing relative module motion. Fig.13 illustrates a typical sudden stop in relative vessel motion in all degrees of freedom indicating succesful connection. Assembly of the final developed system behaved consistently throughout testing. Table 2 shows that the sensed vessel motion after connecting is approximately zero.

Secondly, the system needs to perform motion control in a collaborative manner, where multiple robots work together to achieve a single goal. Centralizing platform control to a single entity facilitated modules contributing to reaching one objective and allowed coordination strategies to increase actuator usage effectiveness. Fig.15 displays responses to reference step changes of a 3x1 lattice configurated platform, showing how the developed system controls to converging and stabilizing at reference state.

The designed framework theoretically supports motion control of any arbitrary configuration, as whas desired. Experiments were conducted on two quite general shapes that both showing satisfactory responses. The control approach adapts to unknown configurations by using scaling rules aimed to be representative over a wide variety of shapes and sizes. Although scaling rules have been designed relying on physics, used assumptions need to be re-evaluated for

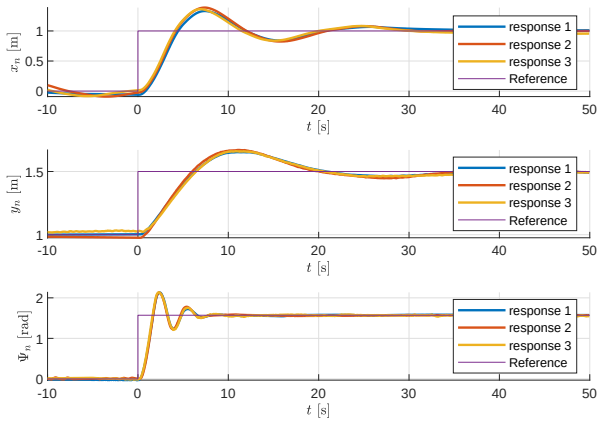

Figure 14: Step responses of single Delfia configuration. Responses are gathered by changing reference of a single degree of motion (x y and yaw) at a time. Three datasets are shown, which show that the responses are rather constant.

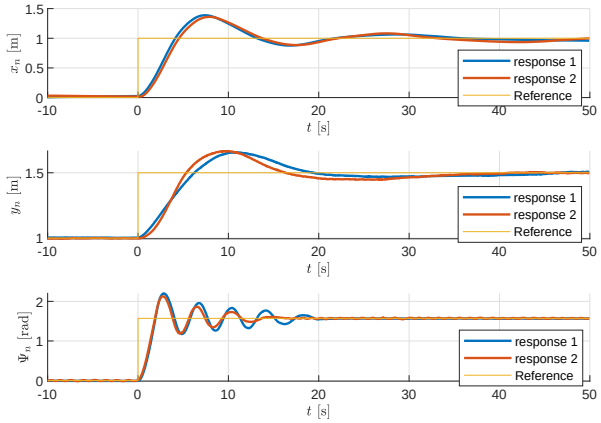

Figure 15: Step responses of a 3x1 lattice configuration. Responses are gathered by changing reference of a single degree of motion (x y and yaw) at a time. Two step responses are shown for each degree of motion.

	Inertia	Maximum input
Single module: Translation	$4.1275kg$	$0.4320N$
Single module: Rotation	$0.1410kgm^2$	$0.0670N * m$
3x1 Conf. Translation	$12.3825kg$	$1.2960N$
3x1 Conf. Rotation	$0.7091kgm^2$	$0.2596Nm$

Table 3: Approximate scaling of reference and assembled configuration

	Rise Time $[s]$	Settling Time $[s]$	Overshoot $[\%]$
Single module	2.5876	27.132	36.0721
3x1 conf.	2.9232	38.2453	37.437
Ratio	1.1297	1.4096	1.0378

Table 4: Comparison between step responses of reference (single vessel) and adapted (3x1) configuration of linear motion in x direction

correctness of future configurations, particularly with more extreme shapes and scales.

5 Conclusion

The discussed criteria on behaviors of self-reconfiguration and collaborative control simultaneously within the same framework are considered achieved. It is concluded that a modular vessel platforming system can be equipped with features automating reconfiguration and collaborative and coordinated control, where the following major challenges are identified as follows;

Firstly, both individual behaviors can already be implemented in a wide variety of approaches, where integration of the two widens the design spectrum significantly more. Both behaviors can be considered complex by themselves, similarly increasing in a combined framework. This complexity toughens challenges of design, but also in facets realizing robustness of a multi-layered system.

Secondly, rarlier developed works showed iterated views on solutions to achieving the desired behaviors. It was found that a main factor for succesful integration is ensuring that both behaviors are interoperable. This particularly means that platform motion control systems need to be able to adapt in real time to configuration changes.

5.1 Discussion

All solutions for subsystems aimed to let the system perform in a lab setting with a fleet of Delfia-1* modules, yet it must be said that these design choices are not optimized or guaranteed to perform on use cases with a different fleet, scale, environment and goals. Replacing or improving components of the system is stimulated by making the control framework as modular as possible. Various subsystems can be further developed, which was expected as exploration of a novel combination of behaviors was the goal rather than optimization. That said, the reader is invited to use the approach and description of implementation for inspiration to develop waterborne multi-vessel collaborative systems.

The approximated platform model relies on the assumptions that either module models remain representative, or that compensating terms can be found. Accelleration dependent contributions of hydrodynamic forces are commonly modelled as constant but inequal in all directions, yielding satisfactory accuracies in most conventional ship use cases [4]. Is questionable to what extent such constant added mass terms remain an accurate model in the scenario of vessel assembly where modules operate in unconventionally close proximity. If (at least some part of) the hydrodynamic forces on a module are accurately represented by this constant directional dependent added mass, then the orientation and placement of that module should be taken into account when estimating contribution to the assembled structure for which the proposed approach on estimating platform model is suitable.

5.2 Recommendations

Firstly, engineers will face similar problems in the future as encountered throughout this work. A framework that allows sharing and integration of solutions to challenges will be key in global development and adoption of automated vessel systems. This would reduce constant re-invention of the wheel would instead allow developers to effectively add development upon existing. ROS is as an impactful standardizer and facilitator of robotic middleware adopted globally. For automated marine systems, an accepted sharing platform for solutions would greatly benefit development, standardization, module reusability interoperability. It is recommended to focus on development and adoption of such a shared platform in successive research built on existing middleware such as a ROS, on others or stand-alone. Key functions and tasks can be further defined and categorized as modules and subfunctions reflecting general marine-control science and industry. Different stakeholders could effectively develop interoperable technical solutions with varying incentives.

Secondly, the amount of works presenting approaches of controlling arbitrary configured modular marine structures is limited, as only Park et al. [9] was found adressing that particular challenge. Many design choices from the system developed in this work are similar to this earlier work, such as adoption of platform-level centralized control topology. Distinction between control effort generation and allocation was already common although this work applied it to a coordinated multi-robot structure. Park et al. [9] also presented the concept of using an approximate platform model estimator, which can be a useful tool supporting platform control performance if the estimation proves of sufficiently accurate. Various facets of this multi-robot collaborative system can be further investigated by searching for fundamental characteristics and common approaches described more broad in general robotic literature.

Collaboration and coordination in a multi-robot structure is aims to increase some facet of the system's performance to increase overall system performance over the sum of individuals. Decentralized topologies could also support such behaviors while reducing single points of failure, although centralization has other benefits.

This work presents a novel platform model based on a combination of module models, assuming that the individual module models are to some extent representative operating in proximity of surrounding modules in a configuration, or that compensating factors can be formulated. Factors that affect accuracy of the combined model need to be investigated. Further developing rules of thumb or approximations performing to reasonably expectable scenarios would be benificial. This can function similar as the concept of hydrodynamic added mass from Humphreys and Watkinson [4], a simplification, yet commonly used in marine control technology providing a great trade-off between simplicity and representativeness. The platform model described in this paper conserves hydrodynamic effects of a module model that show directional dependence, such as hydrodynamic added mass, or dampening models depending on direction of motion. It is important to ask to what extent such models need to be accurate rather than a rough estimate. For future research it is thus suggested to explore benefits of platform model accuracy in use cases of modular marine robotic systems with varying objectives, scenarios and scales. Governing factors affecting vessel platform dynamics can be further investigated. Existing models can be assessed, improved, or new ones can be formed.

References

[1] Fossen, T. I. (2011). *Handbook of marine craft hydrodynamics and motion control*. John Wiley & Sons.

[2] Fossen, T. I. and Fjellstad, O.-E. (1995). Nonlinear modelling of marine vehicles in 6 degrees of freedom. *Mathematical Modelling of Systems*, 1(1):17–27.

[3] Gheneti, B., Park, S., Kelly, R., Meyers, D., Leoni, P., Ratti, C., and Rus, D. (2019). Trajectory planning for the shapeshifting of autonomous surface vessels. In *2019 International Symposium on Multi-Robot and Multi-Agent Systems (MRS)*, pages 76–82.

[4] Humphreys, D. and Watkinson, K. (1978). Prediction of acceleration hydrodynamic coefficients for underwater vehicles from geometric parameters. Technical report, NAVAL COASTAL SYSTEMS LAB PANAMA CITY FL.

[5] Kelly, R. H. (2019). *Algorithms for planning and executing multi-roboat shapeshifting*. PhD thesis, Massachusetts Institute of Technology.

[6] Kirchhoff, G. (1869). Über die bewegung eines rotationskörpers in einer flüssigkeit. *J. Reine Ang. Math*, 71:237–281.

[7] Mateos, L. A., Wang, W., Gheneti, B., Duarte, F., Ratti, C., and Rus, D. (2019). Autonomous latching system for robotic boats. In *2019 International Conference on Robotics and Automation (ICRA)*, pages 7933–7939. IEEE.

[8] O'hara, I., Paulos, J., Davey, J., Eckenstein, N., Doshi, N., Tosun, T., Greco, J., Seo, J., Turpin, M., Kumar, V., et al. (2014). Self-assembly of a swarm of autonomous boats into floating structures. In *2014 IEEE International Conference on Robotics and Automation (ICRA)*, pages 1234–1240. IEEE.

[9] Park, S., Kayacan, E., Ratti, C., and Rus, D. (2019). Coordinated control of a reconfigurable multi-vessel platform: Robust control approach. In *2019 International Conference on Robotics and Automation (ICRA)*, pages 4633–4639. IEEE.

[10] Paulos, J., Eckenstein, N., Tosun, T., Seo, J., Davey, J., Greco, J., Kumar, V., and Yim, M. (2015). Automated self-assembly of large maritime structures by a team of robotic boats. *IEEE Transactions on Automation Science and Engineering*, 12(3):958–968.

[11] Sagatun, S. I. and Fossen, T. I. (1991). Lagrangian formulation of underwater vehicles' dynamics. In *Conference Proceedings 1991 IEEE International Conference on Systems, Man, and Cybernetics*, pages 1029–1034. IEEE.

[12] SNAME, T. (1950). Nomenclature for treating the motion of a submerged body through a fluid. *The Society of Naval Architects and Marine Engineers, Technical and Research Bulletin No*, pages 1–5.

[13] Wang, W., Mateos, L. A., Park, S., Leoni, P., Gheneti, B., Duarte, F., Ratti, C., and Rus, D. (2018). Design, modeling, and nonlinear model predictive tracking control of a novel autonomous surface vehicle. In *2018 IEEE International Conference on Robotics and Automation (ICRA)*, pages 6189–6196.

[14] Wang, W., Shan, T., Leoni, P., Fernández-Gutiérrez, D., Meyers, D., Ratti, C., and Rus, D. (2020). Roboat ii: A novel autonomous surface vessel for urban environments. *arXiv preprint arXiv:2007.10220*.

[15] Yim, M., Shen, W.-M., Salemi, B., Rus, D., Moll, M., Lipson, H., Klavins, E., and Chirikjian, G. S. (2007). Modular self-reconfigurable robot systems [grand challenges of robotics]. *IEEE Robotics & Automation Magazine*, 14(1):43–52.